

Simulation of the neon emission spectrum in a high-frequency discharge and laser fields for transitions with $J = 0.1$

E. V. Koryukina¹ and V. I. Koryukin²

¹Tomsk State University

²Siberian State Medical University, Tomsk

Received March 27, 2008

The dependence of the neon emission spectrum (the dynamic Stark effect and transition probabilities) on the frequency and strength of the electric field generated in a high-frequency discharge at laser excitation was theoretically investigated. The number of regularities in the behavior of the studied characteristics was revealed and investigated. It was shown that the transition probabilities for the Stark energy levels have polynomial dependence on the electric field strength. It was found that the interaction of energy levels in the electric field results in anomalies in the emission spectrum and anisotropy of the transition probabilities.

Introduction

Electric field in a gas discharge and probabilities of transitions are among the most important discharge characteristics. They are used for theoretical study of processes in plasma, as well as for plasma diagnostics. Spectra of rare gases are of special importance, because they are widely used in plasma physics. In particular, the study of rare gas spectra in a circularly polarized alternating electric field, realizable in a high-frequency discharge and at laser excitation, is of current importance. Spectra of atoms in an alternating electric field are determined from the non-stationary Schrödinger equation. Methods for solution of this equation for a circularly polarized alternating electric field and arising problems got prominent coverage in literature.^{1–5}

In this work, the theoretical method, suggested and developed in Refs. 5 and 6, is used to obtain wave functions of atoms in a circularly polarized electric field. This method, free of limitations typical for the perturbation theory, allows investigation of the frequency and electric field strength dependences of shift and splitting of spectral lines of atoms and molecules as well as probabilities of transitions between Stark levels. This work continues a series of works, initiated by the INTAS Project No. 01–0200, where spectra of He,⁷ Ar,⁸ and Kr⁹ atoms were investigated in different ranges of frequency and strength of the electric field.

Method of calculation

In case of circularly polarized electric field, the non-stationary Schrödinger equation is written as

$$i \frac{\partial \psi_n(\mathbf{r}, t)}{\partial t} = [\hat{H}_0(\mathbf{r}) - eF(x \cos \omega t \pm y \sin \omega t)] \psi_n(\mathbf{r}, t), \quad (1)$$

where ψ_n is the wave function of n th system state; $\hat{H}_0(\mathbf{r})$ is the zero-order Hamiltonian; the operator

$-eF(x \cos \omega t \pm y \sin \omega t)$ describes the perturbation, caused by atom interaction with circularly polarized field of the frequency ω and strength F . The signs “+” and “–” correspond to the right and left field polarization, respectively. To pass to the stationary Schrödinger equation, use the rotating wave approximation.¹⁰

To turn to a coordinate system, rotating around the Z -axis with the frequency ω , introduce the wave function in this coordinated system:

$$\varphi(\mathbf{r}, t) = \exp(i\omega t \hat{J}_z) \psi(\mathbf{r}, t), \quad (2)$$

where \hat{J}_z is the z -component of the total angular momentum operator. Substituting wave function (2) into Eq. (1), obtain

$$i \frac{\partial \varphi(\mathbf{r}, t)}{\partial t} = \hat{Q} \varphi(\mathbf{r}, t), \quad \hat{Q} = (\hat{H}_0 - \omega \hat{J}_z \pm F \hat{D}_x). \quad (3)$$

As is seen from Eq. (3), the operator \hat{Q} does not depend on time. Hence, it is possible to pass from non-stationary Schrödinger equation (1) to the stationary one in rotating wave approximation:

$$\hat{Q} \varphi(\mathbf{r}) = \varepsilon \varphi(\mathbf{r}), \quad (4)$$

$$\varphi(\mathbf{r}, t) = \exp(-i\varepsilon t) \varphi(\mathbf{r}), \quad (5)$$

where \hat{Q} is the operator of atom energy in electric field; ε and $\varphi(\mathbf{r}, t)$ are the energy and wave function of the atom in the electric field in the rotating coordinates; they can be found using the time-independent perturbation theory. Within this theory, an approach, suggested and developed in Refs. 5 and 6, is used instead of solving the Schrödinger equation (4).

As is shown in these works, atom wave functions and energies, being solutions of Schrödinger equation (4), are obtained from diagonalization of Q matrix. The matrix can be obtained in representation

of unperturbed wave functions $\varphi_n^{(0)}$, calculated in the absence of external electric field. In such representation, the matrix elements of energy operator \hat{Q} are written as

$$Q_{mm} = E_n^{(0)}\delta_{mm} - \omega \langle \varphi_m^{(0)}(\mathbf{r}) | \hat{J}_z | \varphi_n^{(0)}(\mathbf{r}) \rangle \pm F \langle \varphi_m^{(0)} | \hat{D}_x | \varphi_n^{(0)} \rangle, \quad (6)$$

where $E_n^{(0)}$ is the energy of n th state of an atom in the absence of external electric field; F and ω are the strength and frequency of the external electric field; D_x is the x -component of the dipole transition operator.

Diagonalization of the energy matrix with elements (6) gives a set of wave functions and energy spectrum for n states of an atom in the electric field. After diagonalization of the \hat{Q} matrix, obtain the energies ε_n and wave functions in the form

$$\varphi_n(\mathbf{r}, t) = \exp(-i\varepsilon_n t) \sum_k C_{nk} \varphi_k^{(0)}(\mathbf{r}) \quad (7)$$

for n states of an atom in the external electric field in the rotating coordinates. The coefficients C_{nk} in wave function (7) depend on the frequency and strength of the external electric field. To find average energies of an atom in the initial system of coordinates, the averaging over vibration period is required. Then the average energy of the system in electric field in the initial system of coordinates is defined as

$$\begin{aligned} \bar{E}_n &= \langle \varphi_n(\mathbf{r}, t) | H(\mathbf{r}, t) | \varphi_n(\mathbf{r}, t) \rangle = \\ &= \varepsilon_n + \omega \langle \varphi_n(\mathbf{r}) | \hat{J}_z | \varphi_n(\mathbf{r}) \rangle. \end{aligned} \quad (8)$$

As it follows from Eq. (8), \bar{E}_n is time-independent.

Matrix elements of the D_x operator are defined as

$$\begin{aligned} \langle \varphi_m^{(0)} | \hat{D}_x | \varphi_n^{(0)} \rangle &= \langle \gamma JM | D_x | \gamma' J' M' \rangle = \\ &= \frac{(-1)^{J-M}}{\sqrt{2}} \left[\begin{pmatrix} J & 1 & J' \\ -M & -1 & M' \end{pmatrix} - \begin{pmatrix} J & 1 & J' \\ -M & 1 & M' \end{pmatrix} \right] \langle \gamma J \| D \| \gamma' J' \rangle, \end{aligned} \quad (9)$$

where the reduced matrix elements $\langle \gamma J \| D \| \gamma' J' \rangle$ are calculated depending on the type of coupling. For Ne atom, the JL -coupling is realizable. The calculation of $\langle \gamma J \| D \| \gamma' J' \rangle$ is given in Refs. 8 and 9 in more detail.

Again, the wave functions and energies, determined from the diagonalization of the \hat{Q} matrix, are used for calculation of spontaneous-transition probabilities in electric field. The probability of spontaneous photon emission into the element of solid angle $d\Omega$ at transition from $|n\rangle$ to $|m\rangle$ state with the polarization \mathbf{e}_q is defined by the equation:

$$A_q = \frac{\omega^3}{hc^3} |\mathbf{e}_q \langle \Psi_n | \mathbf{D} | \Psi_m \rangle|^2 d\Omega, \quad (10)$$

where ω is the transition frequency; \mathbf{e}_q is the polarization vector; $\mathbf{D} = -e \sum_i \mathbf{r}_i$ is the dipole moment

of atom; Ψ_n and Ψ_m are the wave functions of n th and m th states of atom in the external electric field. Based on Eq. (10), the probability of transition from n to m state for the radiation, polarized in \mathbf{e}_q direction and averaged over all possible \mathbf{D} -space orientations, is calculated by the equation

$$A_{nm} = \frac{4\omega^3}{3hc^3} \sum_q |\langle \Psi_n | D_q | \Psi_m \rangle|^2, \quad (11)$$

where D_q are the cyclic components of the vector \mathbf{D} . The wave functions Ψ_n and Ψ_m are determined from the diagonalization of the energy matrix \hat{Q} with matrix elements (6). Substituting the wave functions Ψ_n and Ψ_m in Eq. (11) and using the Wigner–Eckart theorem, obtain the following form of the equation for the probability of $JM \rightarrow J'M'$ transition between magnetic substates:

$$\begin{aligned} A(JM \rightarrow J'M') &= \frac{4\omega_{JM,J'M'}^3}{3hc^3} |D_{JM,J'M'}|^2, \\ D_{JM,J'M'} &= \sum_q \left| \sum_{ij} C_i^{(JM)*} C_j^{(J'M')} (-1)^{J_i - M_i} \begin{pmatrix} J_i & 1 & J_j \\ -M_i & q & M_j \end{pmatrix} \right. \\ &\quad \left. \times \langle \gamma_i J_i \| D \| \gamma_j J_j \rangle \right|^2, \end{aligned} \quad (12)$$

where $C_i^{(JM)}$ and $C_j^{(J'M')}$ are the coefficients of expansion of wave functions for an atom in the field in unperturbed wave functions $\varphi_j^{(0)}(\gamma_j J_j M_j)$; $\omega_{JM,J'M'}$ is the frequency of the $JM \rightarrow J'M'$ transition.

Existing experimental techniques do not usually allow the splitting between magnetic substates to be measured and corresponding transition probabilities to be determined; hence, it is necessary to calculate the probabilities of $J \rightarrow J'$ transitions between states. These probabilities are calculated by the equation

$$A(J \rightarrow J') = \frac{1}{2J+1} \sum_{MM'} A(JM \rightarrow J'M'). \quad (13)$$

Consider the results obtained within this theoretical approach.

Discussion of the results

The above-described method was used for Ne spectrum simulation in a high-frequency discharge and laser fields. In \hat{Q} calculation, ns , np , nd , and nf states with $n \leq 10$ were taken into account. Thus, 267 energy levels (1309 magnetic substates) were taken into account when calculating the Ne atom energy matrix in the electric field. Transitions between Stark levels with $J, J' = 0.1$ were studied. The electric field strength up to 10 kV/cm was considered at frequencies: $\omega = 100$ MHz for a high-frequency discharge,¹²

$\omega = 151.31 \cdot 10^3$ MHz for the NH_3 laser, and $\omega = 243.52 \cdot 10^4$ MHz for the HCN laser.¹³ Spectral lines in the Visible were mainly considered.

First, two possible variants of behavior of spectral lines in electric field were revealed on the base of the calculations. The first variant is shown by the lines, corresponding to the $nl'_1[K_1]J_1M_1 \rightarrow ml'_2[K_2]J_2M_2$ transitions. These lines in electric field are shifted proportional to F^2 and splitted; the split decreases with field frequency rise. The spectral lines, corresponding to transitions from M to $+M'$ and $-M'$ states, coincide. As follows from the analysis of wave functions, such behavior is explained by the fact that the energy levels $nl'[K]JM$, even very high, virtually do not mix with the neighboring levels under the effect of electric field.

The second variant of behavior is observed for the spectral lines corresponding to the $nl_1[K_1]J_1M_1 \rightarrow ml_2[K_2]J_2M_2$ transitions. In contrast to the first variant, the $nl[K]JM$ levels mix in electric field, and the mixing degree increases with the base quantum number n of the energy level, from which the transition to lower states occurs. In addition, the mixing degree of Stark levels increases with the strength of electric

field and strongly depends on its frequency. As a result of this mixing, the spectral lines, corresponding to transitions from M to $+M'$ and $-M'$ states, do not coincide any more. In weak interaction of Stark levels, the shift of $nl_1[K_1]J_1M_1 \rightarrow ml_2[K_2]J_2M_2$ lines is still quadratic in the electric field strength, while an increase of the filed frequency results in a decrease of shift and split of Ne atom energy levels. Strong interaction of energy levels results in a break of the quadratic dependence of spectral line shifts on field strength, anomalies in the emission spectrum, and the appearance of forbidden lines. The strongest mixing of substates is observed for the spectral lines $nd[K_1]J_1M_1 \rightarrow mp[K_2]J_2M_2$, since the $nd[K]JM$ states have a significant admixture of $nf[K]JM$ states, and the $np[K]JM$ states – of $nd[K]JM$ ones.

To illustrate all the mentioned above, figure 1 shows the shift and split of spectral lines $9s[3/2]_1-3p[3/2]_1$ and $7d[3/2]_1-3p[1/2]_1$ for the Ne atom in electric field of different frequencies. The shift of Stark levels in the filed is defined as $\Delta E = E - E_0$, where E and E_0 are positions of a considered line in electric field and in the absence of filed, respectively. Similar results (see Fig. 1) are obtained for all studied lines.

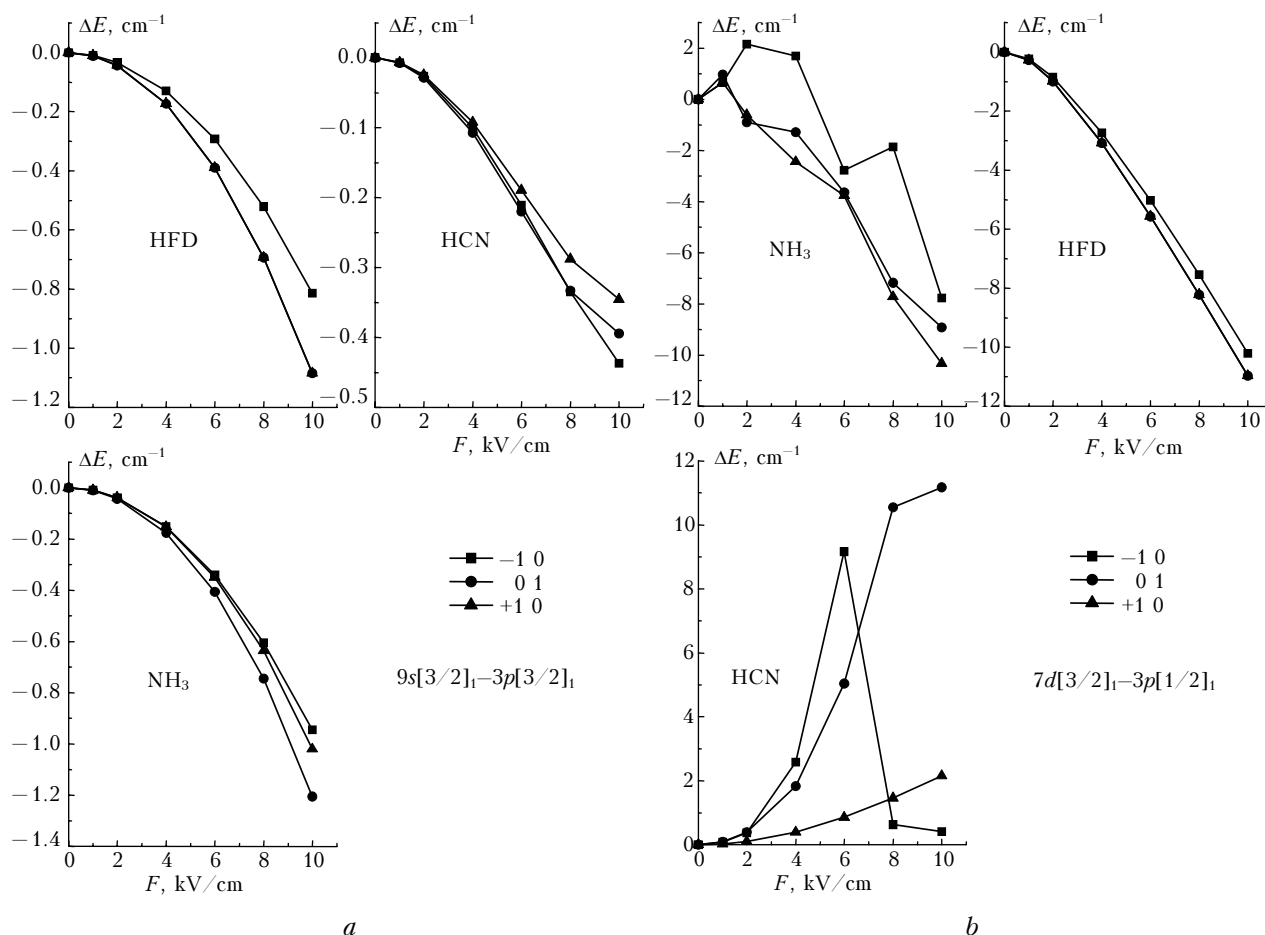


Fig. 1. The Stark effect as a function of electric field frequency and strength: the spectral line $\lambda = 455.387$ nm (weak mixing of substates) (a) and 426.892 nm (strong mixing) (b).

Then the calculated wave functions and atom energies in the field were used to study the dependence of transition probabilities in the Ne spectrum on frequency and strength of the electric field. Comparison of transition probabilities, calculated in the absence of electric field, with the accurate data¹⁴ (Table 1) shows their good agreement, which confirms the reliability of the calculation method.

Table 1. Probabilities of $n'lJM-n'l'J'M'$ transitions in the absence of electric field, 10^6 s^{-1}

Transition $i \rightarrow k$	λ , nm	A_{ik}	
		This work	Ref. 14
$5d[3/2]_i-3p[3/2]_i$	515.586	1.80	1.9
$5d'[3/2]_i-3p'[3/2]_i$	512.193	0.58	0.56
$4d[3/2]_i-3p[3/2]_i$	591.527	4.60	4.5
$4d[1/2]_i-3p[1/2]_0$	622.746	2.18	2.4
$5d[1/2]_i-3p[1/2]_i$	471.018	3.52	4.2
$4p[1/2]_i-3s[1/2]_i$	359.466	0.87	0.66
$5d'[3/2]_i-3p'[1/2]_i$	512.193	1.07	1.3
$4d'[1/2]_i-3p'[1/2]_i$	534.258	8.41	11
$5s[3/2]_i-3p[1/2]_i$	566.412	0.52	0.69

After testing the calculation accuracy, the probabilities of $n'lJM-n'l'J'M'$ transitions between Stark levels in the electric field of different strengths and frequencies were calculated by Eq. (12) within the suggested method. The obtained results are given in Table 2.

As it follows from Table 2, the probabilities of all $n'l_1[K_1]J_1M_1 \rightarrow m'l_2[K_2]J_2M_2$ transitions are virtually insensitive to variations of electric field frequency and strength. The probabilities of the majority of these transitions decrease with growth of the electric field strength, and transition from the Stark level to levels with $+M$ and $-M$ quantum numbers have either the same or similar probabilities.

The probabilities of $n'l_1[K_1]J_1M_1 \rightarrow m'l_2[K_2]J_2M_2$ transitions behave just different. Even at weak mixing of Stark levels of this type, transition probabilities depend on electric field strength and frequency. At a high degree of the energy level mixing, the probabilities of transitions between Stark levels can both decrease and increase with the electric field strength. In this case, transitions from one energy substate to others with the quantum numbers $+M$ and $-M$ usually have different probabilities. Thus, anisotropy is observed for probabilities of $n'l_1[K_1]J_1M_1 \rightarrow m'l_2[K_2]J_2M_2$ transitions, which can be quite significant. To illustrate this, figure 2 shows the dependence of transitions probabilities between magnetic substates on electric field frequency and strength for the $7d[3/2]_i-3p[1/2]_i$ spectral line.

Similar dependences were obtained for other spectral lines.

The $J \rightarrow J'$ transitions have been studied in the same way. The probabilities $A_{JJ'}$ have been calculated by Eq. (13) at different values of the electric field strength and frequency. The results for the spectral lines $8d[1/2]_0-3p[3/2]_i$ (with weak mixing of energy sublevels) and $7d[1/2]_0-3p[3/2]_i$ (with strong mixing) are shown in Fig. 3.

In case of weak sublevel interaction, the probabilities $A_{JJ'}$ evidently smoothly decrease with an increase of electric field strength (Fig. 3a) and the field strength dependence of $A_{JJ'}$ is of polynomial character. In a high-frequency discharge, the polynomial is cubic:

$$A_{JJ'} = a + bF + cF^2 + dF^3,$$

while it is quartic at the NH_3 laser frequency:

$$A_{JJ'} = a + bF + cF^2 + dF^3 + eF^4.$$

Table 2. Probabilities of $n'lJM-n'l'J'M'$ transitions in a high-frequency discharge and laser fields (NH_3 - and HCN lasers), 10^6 s^{-1}

Transition $i \rightarrow k$	λ , nm (at $F = 0$)	A_{ik} (at $F = 0$)	ω	$M \rightarrow M'$	A_{ik}		
					$F = 2 \text{ kV/cm}$	$F = 10 \text{ kV/cm}$	
$9s[1/2]_0-3p[1/2]_i$	458.428	0.246	HFD	$0 \rightarrow \pm 1$	0.082	0.082	
			NH_3	$0 \rightarrow \pm 1$	0.082	0.082	
			HCN	$0 \rightarrow +1$	0.082	0.084	
$9p[1/2]_0-3s[1/2]_i$	268.755	0.113	HFD	$0 \rightarrow \pm 1$	0.038	0.036	
			NH_3	$0 \rightarrow \pm 1$	0.038	0.036	
			HCN	$0 \rightarrow \pm 1$	0.037	0.036	
$9d[3/2]_i-3p[1/2]_0$	490.676	0.079	HFD	$0 \rightarrow \pm 1$	0.079	0.078	
			NH_3	$0 \rightarrow \pm 1$	0.079	0.078	
			HCN	$0 \rightarrow \pm 1$	0.079	0.078	
$9s[3/2]_i-3p[3/2]_i$	455.387	0.223	HFD	$+1 \rightarrow 0$	0.112	0.113	
				$-1 \rightarrow 0$	0.112	0.110	
				$0 \rightarrow \pm 1$	0.112	0.110	
				NH_3	$\pm 1 \rightarrow 0$	0.112	0.111
				$0 \rightarrow \pm 1$	0.112	0.109	
				HCN	$\pm 1 \rightarrow 0$	0.112	0.112
$0 \rightarrow \pm 1$	0.110	0.110					

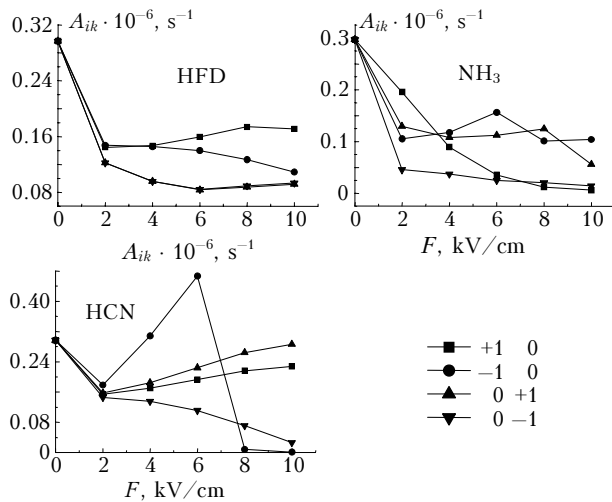


Fig. 2. Transition probabilities as functions of electric field frequency and strength for the $7d[3/2]_1-3p[1/2]_1$ spectral line at $\lambda = 426.892$ nm.

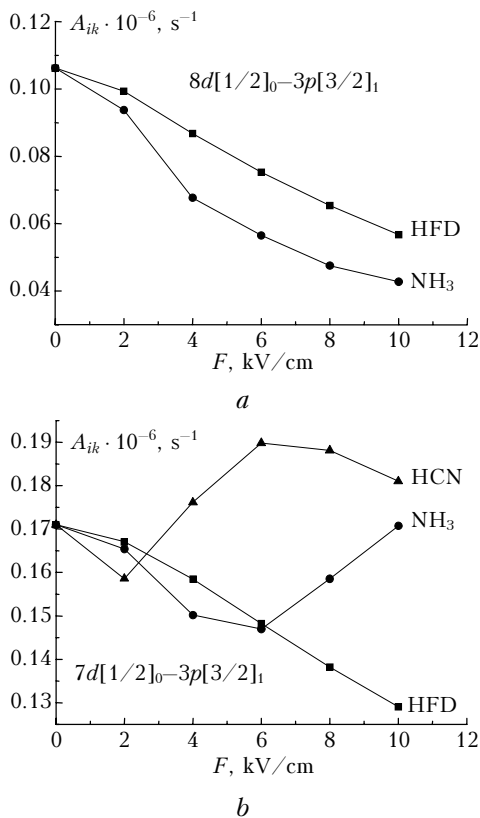


Fig. 3. The transition probabilities $A_{JJ'}$ as functions of electric field frequency and strength for the spectral line $\lambda = 452.924$ nm (weak sublevel mixing) (a) and 426.892 nm (strong sublevel mixing) (b).

As is expected, the probabilities of $J \rightarrow J'$ transitions in case of strong interaction of sublevels (Fig. 3b) both increase and decrease with growth of electric field strength at different field frequencies. However, they still satisfy the found polynomial dependences, i.e., a cubic polynomial in a high-frequency discharge and quartic one at the NH_3 laser

frequency; at the HCN-laser frequency the curve of probability variation is well approximated by the quartic polynomial.

Based on previous investigations,^{7,9} one can suppose that the order of the polynomial will further increase by unity when increasing the electric field frequency to 10^7 MHz, i.e., $A_{JJ'} = a + bF + cF^2 + dF^3 + eF^4 + fF^5$. The same polynomial dependences have been obtained for all studied transition probabilities. Regularities, obtained in simulating the Ne spectrum, are in very well agreement with the earlier obtained⁷⁻⁹ simulation results of emission spectra of He, Ar, and Kr gases.

Conclusion

The general analysis of the calculations allows revealing of a series of regularities for the Ne emission spectrum in a high-frequency discharge and the laser fields. It is shown that the spectral lines corresponding to the $nl'_1[K_1]J_1M_1 \rightarrow ml'_2[K_2]J_2M_2$ and $nl_1[K_1]J_1M_1 \rightarrow ml_2[K_2]J_2M_2$ transitions behave absolutely different when varying both strength and frequency of the external electric field. An increase in the electric field strength results in ordinary shift and splitting of spectral lines corresponding to the transitions $nl'_1[K_1]J_1M_1 \rightarrow ml'_2[K_2]J_2M_2$. The line shift is proportionate to F^2 , splitting of levels decreases with the growth of the field frequency. At the same time, an increase in electric field strength and frequency for the spectral lines, corresponding to the $nl_1[K_1]J_1M_1 \rightarrow ml_2[K_2]J_2M_2$ transitions, results in anomalies in shift and splitting of these lines. The reason of such different behavior is the difference in the degree of energy level mixing in the electric field.

The same reason is in the base of the difference in behavior of transition probabilities when varying electric field frequency and strength. The probabilities of $nl'_1[K_1]J_1M_1 \rightarrow ml'_2[K_2]J_2M_2$ transitions are virtually independent of electric field frequency and strength and equally probable for the $M \rightarrow \pm M'$ transitions, while the probabilities of $nl_1[K_1]J_1M_1 \rightarrow ml_2[K_2]J_2M_2$ transitions can both decrease and increase with growth of field strength and frequency. Strong interaction of energy levels results in anisotropy of $nl_1[K_1]J_1M_1 \rightarrow ml_2[K_2]J_2M_2$ transition probabilities. Finally, the polynomial dependence of $J \rightarrow J'$ transition probabilities on electric field strength is found, and the order of the polynomial increases with the field frequency.

The obtained theoretical results can be used to explain physical processes in plasma, generated in a circularly polarized alternating electric field. In particular, the calculated data allows the electric field strength inside a discharge to be found, the mechanisms of excited level populating and reasons of spectral line intensity variation to be clarified. In addition, the obtained regularities can also be useful in the modeling of new light and excitation sources.

References

1. N.B. Delone and V.P. Krainov, *Phys.-Uspekhi* **169**, No. 7, 753–772 (1999).
2. N.B. Delone and V.P. Krainov, *Atom in a Strong Light Field* (Energoatomizdat, Moscow, 1978), 288 pp.
3. N.L. Manakov, L.B. Rapoport, and A.G. Fanshtein, *Teor. Mat. Fiz.* **30**, No. 3, 395–407 (1977).
4. L.B. Rapoport, B.A. Zon, and N.L. Manakov, *Theory of Multiphoton Processes in Atoms* (Atomizdat, Moscow, 1978), 182 pp.
5. E.V. Koryukina, *Izv. Vyssh. Uchebn. Zaved. Ser. Fizika*, No. 9, 3–11 (2005).
6. E.V. Koryukina, *Atmos. Oceanic Opt.* **17**, Nos. 2–3, 131–135 (2004).
7. E.V. Koryukina, *Atmos. Oceanic Opt.* **19**, No. 7, 519–525 (2006).
8. E.V. Koryukina, *J. Phys. D* **38**, No. 17, 3296–3303 (2005).
9. E.V. Koryukina, *Proc. SPIE* **6263**, 175–185 (2006).
10. F.V. Bunkin and A.M. Prokhorov, *Zh. Eksp. Teor. Fiz.* **46**, No. 3, 1091–1097 (1964).
11. A.P. Yutsis and A.Yu. Savukinas, *Mathematical Foundations of Atom Theory* (Mokslas, Vilnius, 1973), 479 pp.
12. A. Skudra and G. Revalde, *J. Quant. Spectrosc. and Radiat. Transfer* **61**, No 6, 717–728 (1999).
13. A.M. Prokhorov, *Lasers Handbook. V. 1* (Sov. Radio, Moscow, 1978), 504 pp.
14. <http://www.nist.gov>